Adv. Electron. Mater. **2020**, *6*, 2000721
ADVANCED ELECTRONIC MATERIALS
www.advelectronicmat.de

Multifunctional Protein Nanowire Humidity Sensors for Green Wearable Electronics

*Xiaomeng Liu, Tianda Fu, Joy Ward, Hongyan Gao, Bing Yin, Trevor Woodard, Derek R. Lovley, and Jun Yao**

X. Liu, T. Fu, H. Gao, Dr. B. Yin, Prof. J. Yao
Department of Electrical and Computer Engineering
University of Massachusetts
Amherst, MA 01003, USA
J. Ward, T. Woodard, Prof. D. R. Lovley
Department of Microbiology
University of Massachusetts
Amherst, MA 01003, USA
Prof. D. R. Lovley, Prof. J. Yao
Institute for Applied Life Sciences (IALS)
University of Massachusetts
Amherst, MA 01003, USA

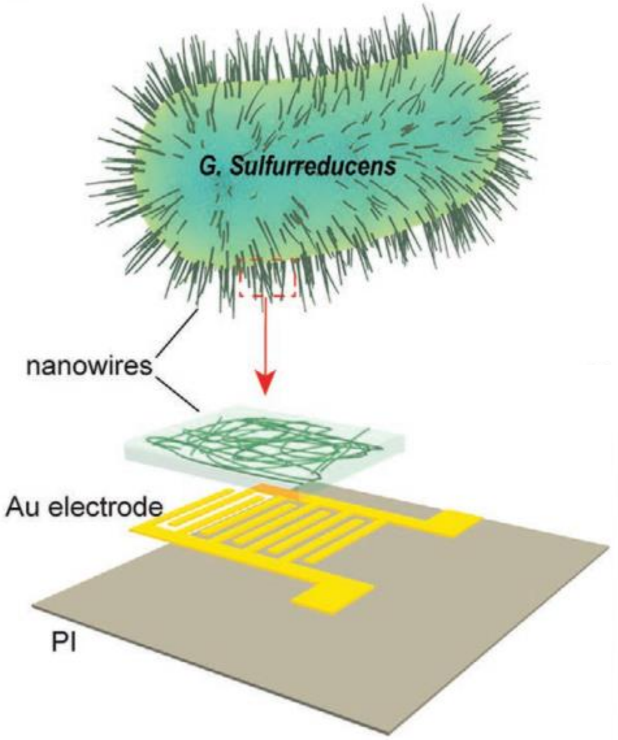

S JENIFER
03.04.2021

FULL PAPER

NANO · MICRO small

Biosynthetic Nanocomposites

www.small-journal.com

Conductive Composite Materials Fabricated from Microbially Produced Protein Nanowires

Yun-Lu Sun, Hai-Yan Tang, Alexander Ribbe, Volodimyr Duzhko, Trevor L. Woodard, Joy E. Ward, Ying Bai, Kelly P. Nevin, Stephen S. Nonnenmann, Thomas Russell, Todd Emrick, and Derek R. Lovley**

- e-pilus: pilus that is sufficiently electrically conductive along its length to promote long-range electron exchange between the microbe expressing e-pili and the external environment.
- e-PNs of *Geobacter sulfurreducens* conduct electrons over micrometer-scale distances.

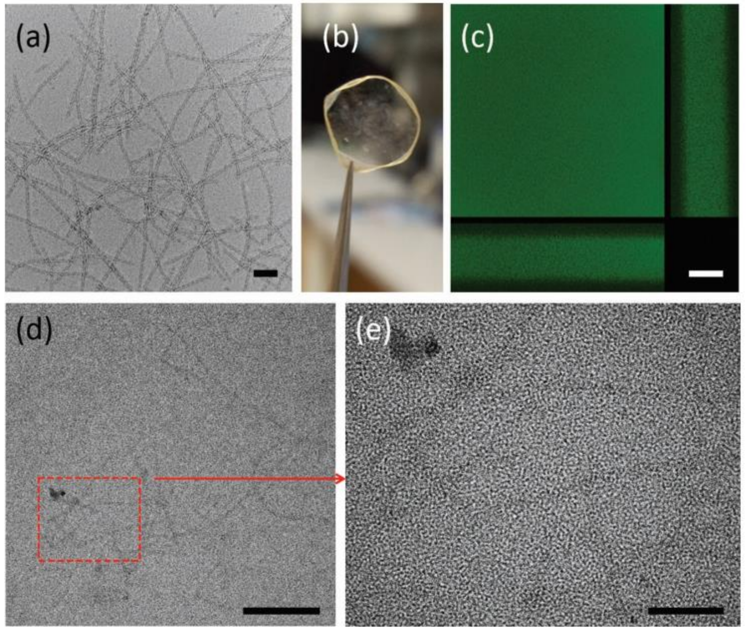

Figure 1. Visualization of purified e-PNs and e-PN/PVA composites. a) Transmission electron micrograph (TEM) of e-PNs after dropcasting

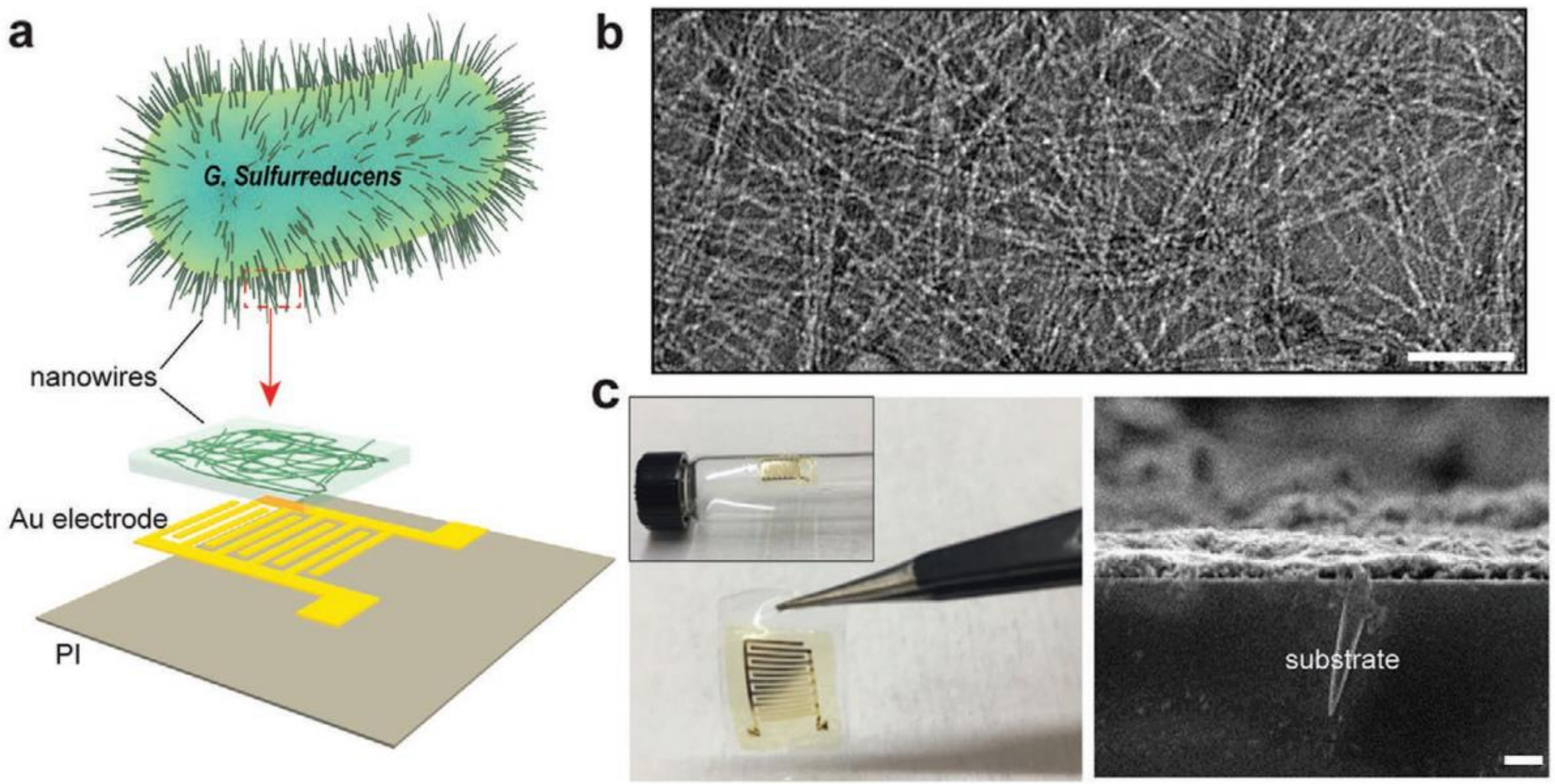

a) (Top) Schematic of microorganism *Geobacter sulfurreducens* with outer-membrane protein nanowires, and (bottom) schematic of the sensor device made from harvested protein nanowires.

b) TEM images of purified protein nanowires. Scale bar, 100 nm.

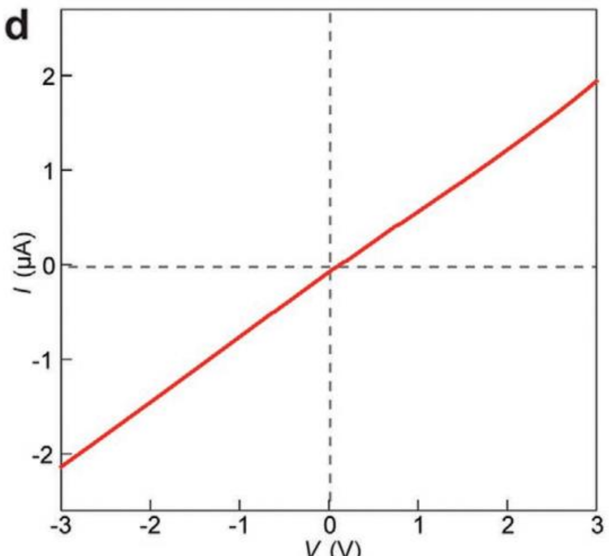

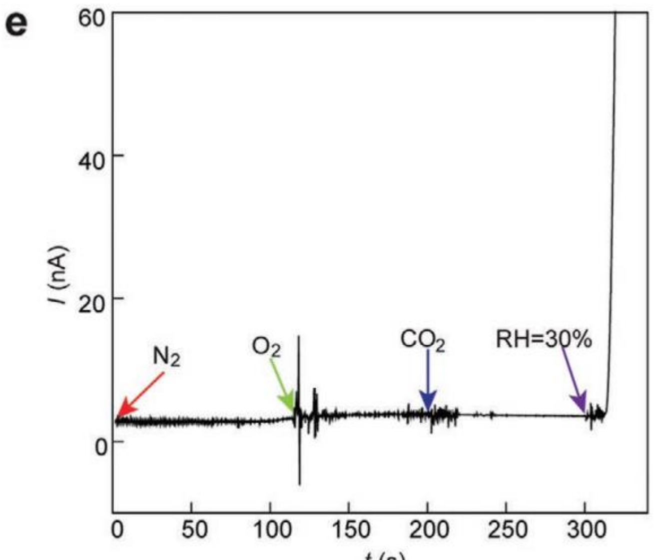

d) Representative *I*–*V* curve recorded from a protein nanowire device under ambient environment (RH = 50%).

e) Current response from a protein nanowire device to atmospheric gases. A voltage bias of 1 V was applied to the device. The baseline current was measured at RH = 5%, so here the relative signal change ($\Delta I/I$) at RH = 30% was higher than that in Figure 2a using a baseline current measured at RH = 20%.

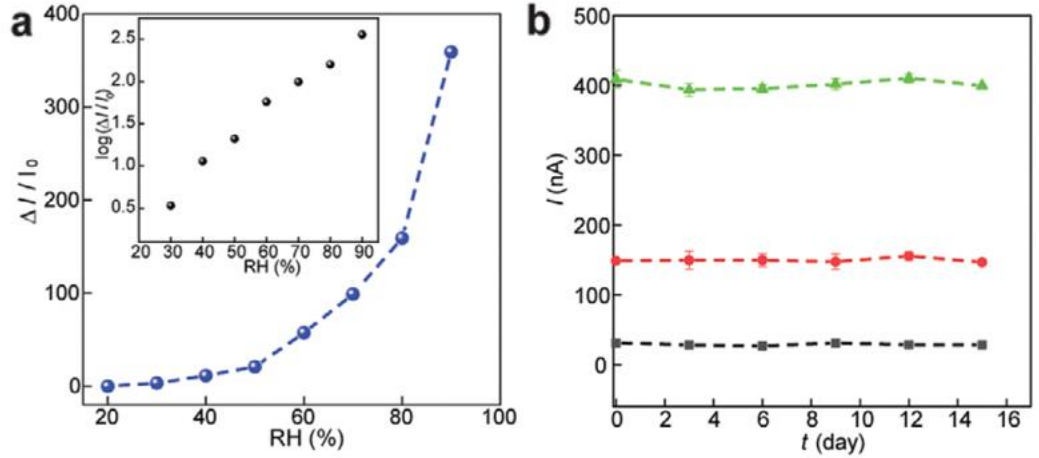

a) Relative current change ($\Delta I/I_0$) in the nanowire device with respect to the relative humidity (RH). I_0 is the baseline current measured at RH = 20%. The inset shows the logarithmic scale. b) A half-month continuous measurement of the current (I) in a same device at RH of 40% (gray), 60% (red), and 80% (green).

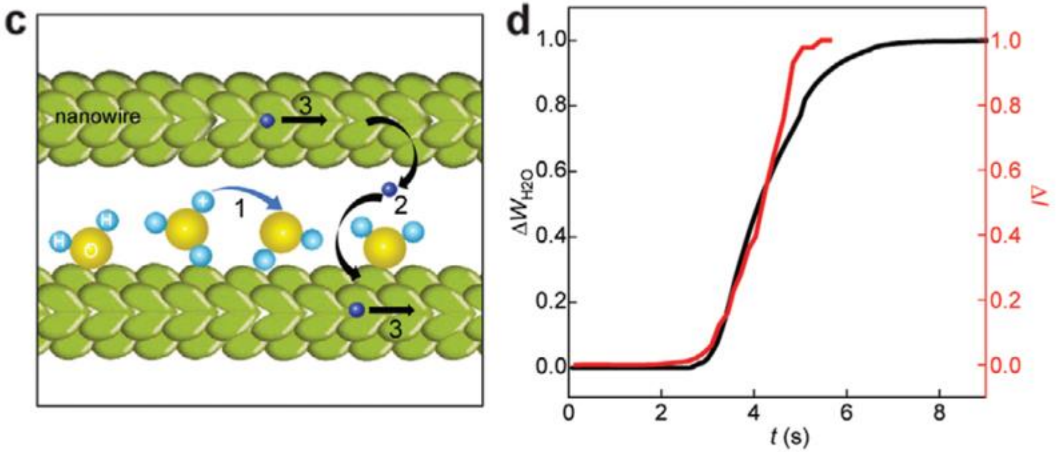

c) Multiple charge (blue dots) transfer processes indicate the general external ionic conduction, interwire conduction, and intrawire conduction, respectively. d) Temporal correlation between moisture adsorption (ΔWH2O, black curve) in a protein nanowire film and current change (ΔI, red curve) in a nanowire device when RH changed from 30% to 90% by bubbling. The values are normalized.

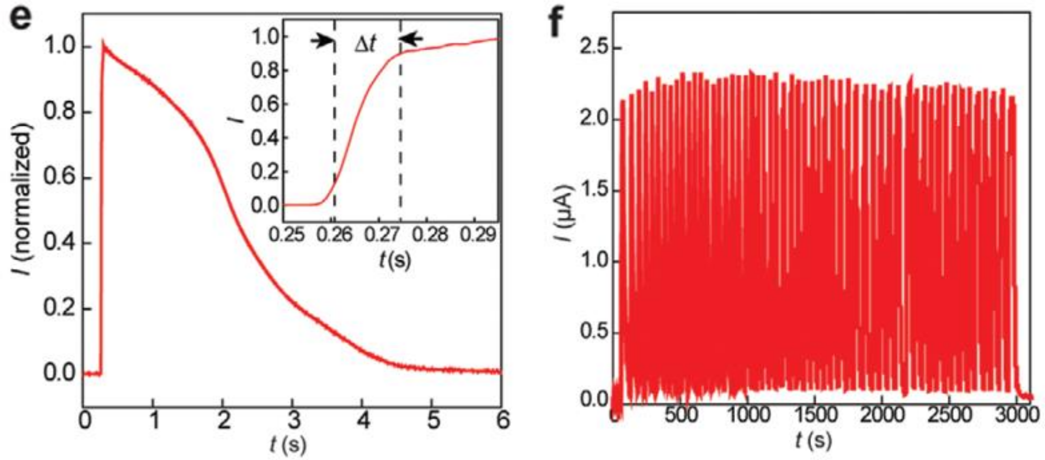

e) Sensor response to an instant RH change from 30% to 90%. The inset shows the response time (Δt), defined as the rising time from 10% to 90% of the signal peak. f) Sensor response to 55 repeated RH changes from 40% to 90%.

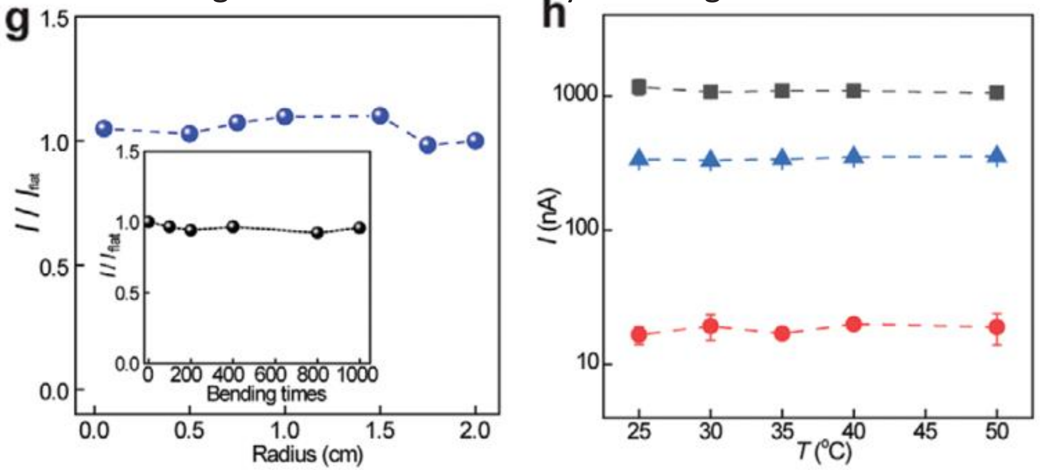

g) Sensor current (I) at different bending radii with respect to current (I_{flat}) measured at flat state. (Inset) sensor current in repeated bending test at a bending radius of 0.5 mm. h) Current (I) from a sensor in the temperature range of 25–50 °C, measured at RH of 40% (red), 60% (blue), and 90% (gray). All the data were obtained at a bias of 1 V.

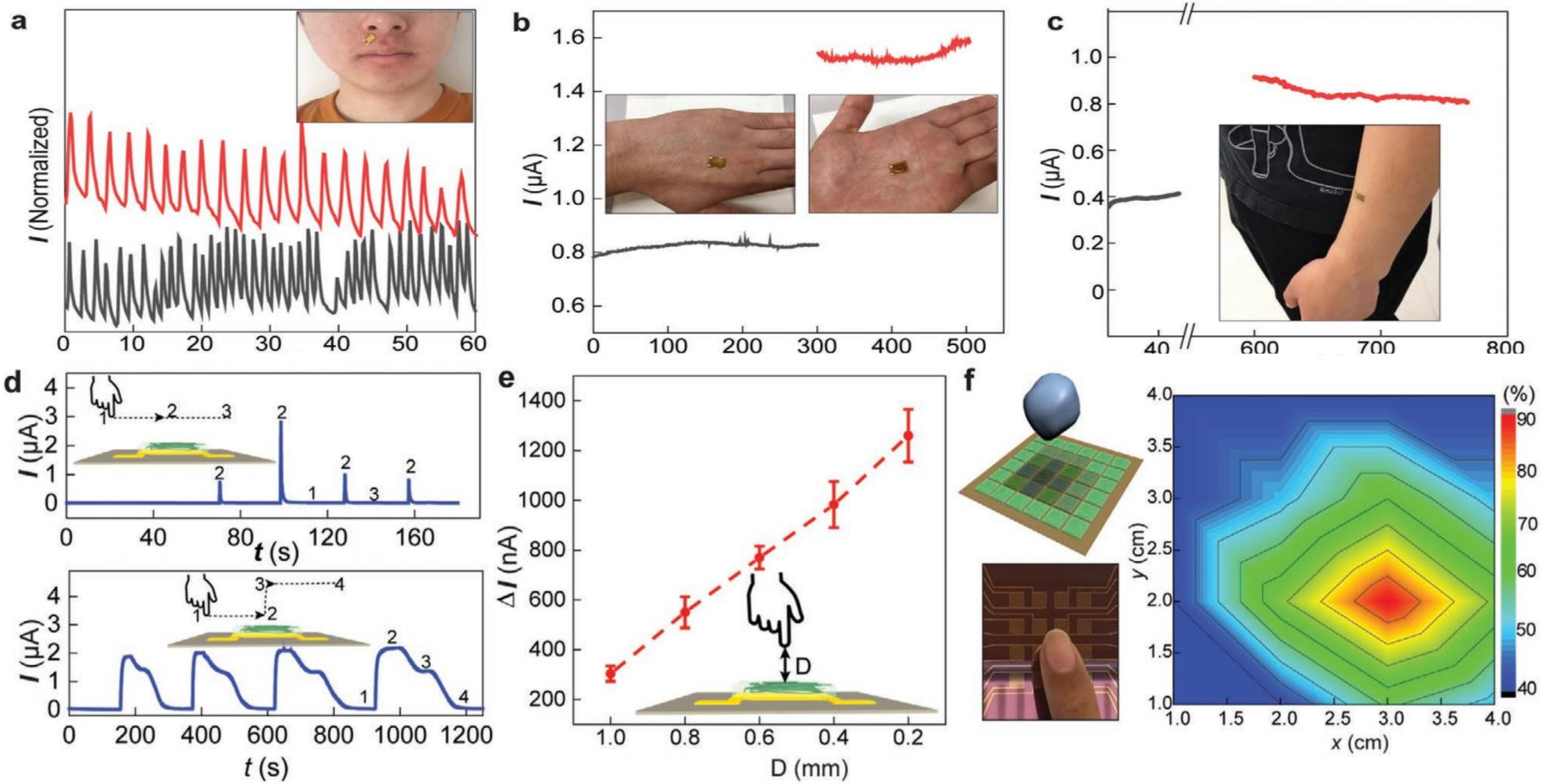

a) Current responses from a protein nanowire device placed close to the nose, measured at (red) normal state and (gray) after exercise. b) Current responses from a protein nanowire device placed on the hand palm (gray curve) and on the back of the hand (red line). c) Current responses from a protein nanowire device placed on the arm (gray) before and (red) after exercise. d) Current responses from a protein nanowire device to repeated (four times) finger movements of (top) swiping across and (bottom) gradual elevating. The insets show the schematics of finger track, with the numbers indicating the positions.

Current generation in an unbiased protein nanowire device exposed to a humidity gradient

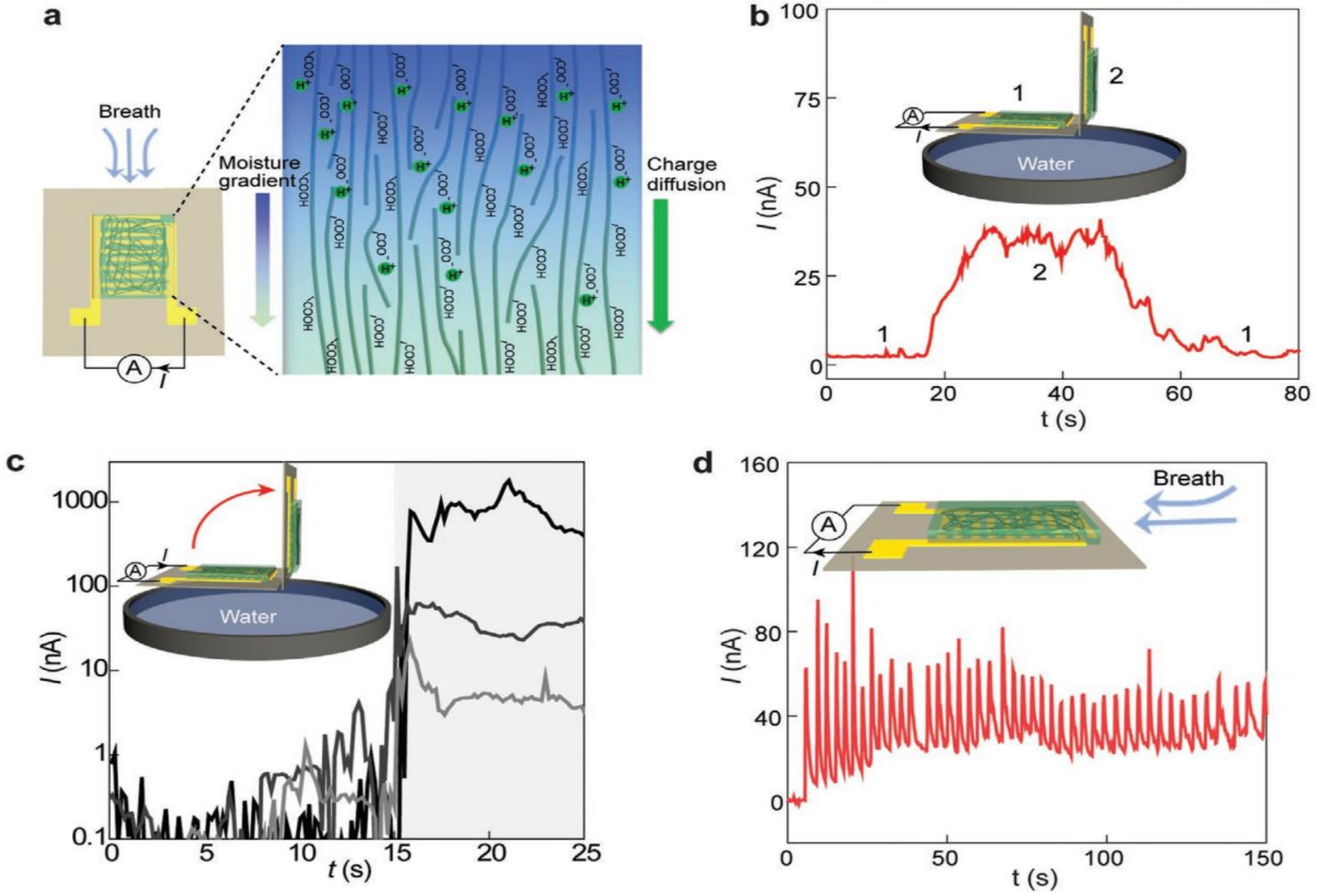

a) Schematic of the current generation in an unbiased protein nanowire device exposed to a humidity gradient (e.g., upon a breath). The humidity gradient induces a moisture-adsorption gradient in the film, which further generates an ionization gradient. The ionization gradient leads to a gradient in the mobile charge species (e.g., protons against an immobile background COOH-), which diffuse to generate current. b) A nanowire device placed in a vertical position with respect to the water surface (inset) produced more current than that in a horizontal position. c) Generated currents (*t* > 15) in unbiased protein nanowire sensors by rotating the devices from a horizontal position to vertical position with respect to the water surface (inset). The protein nanowire films were prepared at pH of 2 (black curve), 7 (dark gray), and 10 (gray), respectively. d) An unbiased protein nanowire device served as a self-powered respiratory sensor by converting the humidity gradient of a breath into a current spike.

Device fabrication process.

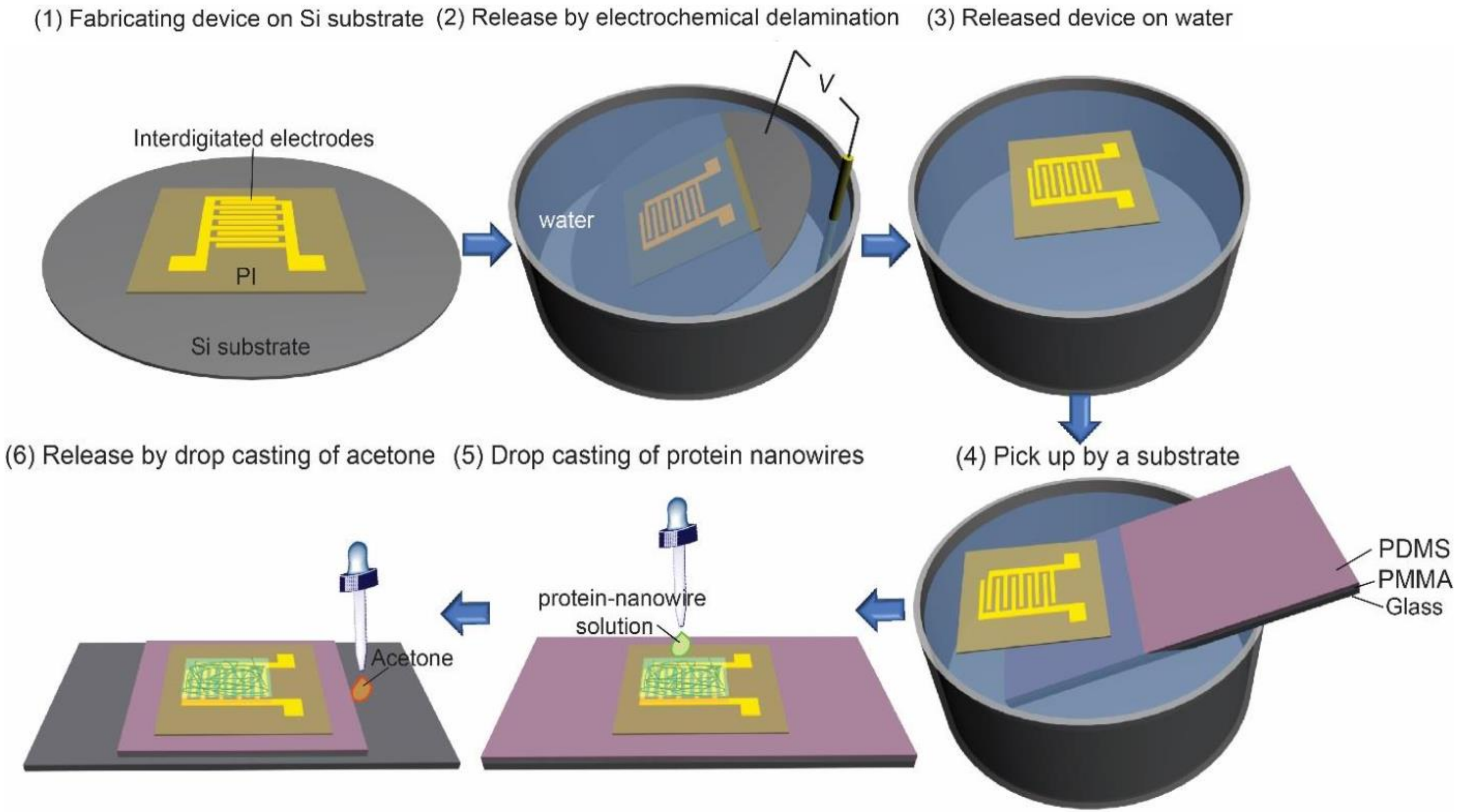

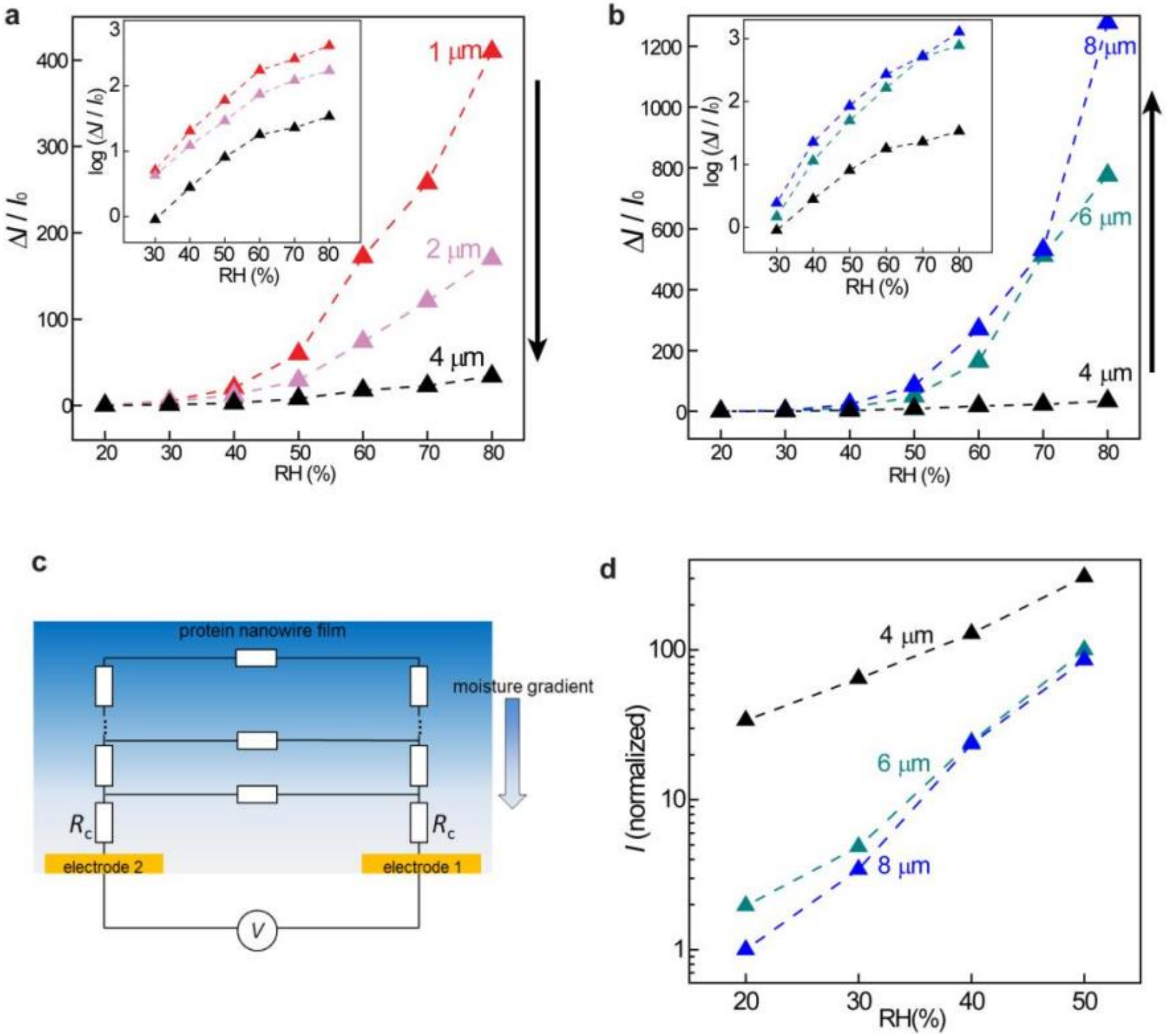

Film-thickness dependence in sensor response. (**a**) Relative current change (Δ*I*/*I*o) (*I*o measured at a baseline RH of 20%) in protein nanowire sensors with film thickness of 1 µm (red), 2 µm (purple), and 4 µm (black), respectively. Inset shows the logarithmic plot. A decrease in sensor response was observed with the increase in nanowire film thickness. (**b**) Δ*I*/*I*o in protein nanowire sensors with film thickness of 4 µm (black), 6 µm (cyan), and 8 µm (blue), respectively. Inset shows the logarithmic plot. An increase in sensor response was observed with the increase in nanowire film thickness. (**c**) Cross-section schematics of a protein nanowire device and the equivalent circuit. The opposite trend in thick film can be understood from the existence of a vertical moisture gradient in the protein nanowire film. (**d**) The analysis in (c) was supported by the observation that the overall device conduction decreased with the increase in film thickness at low RH≤ 50%

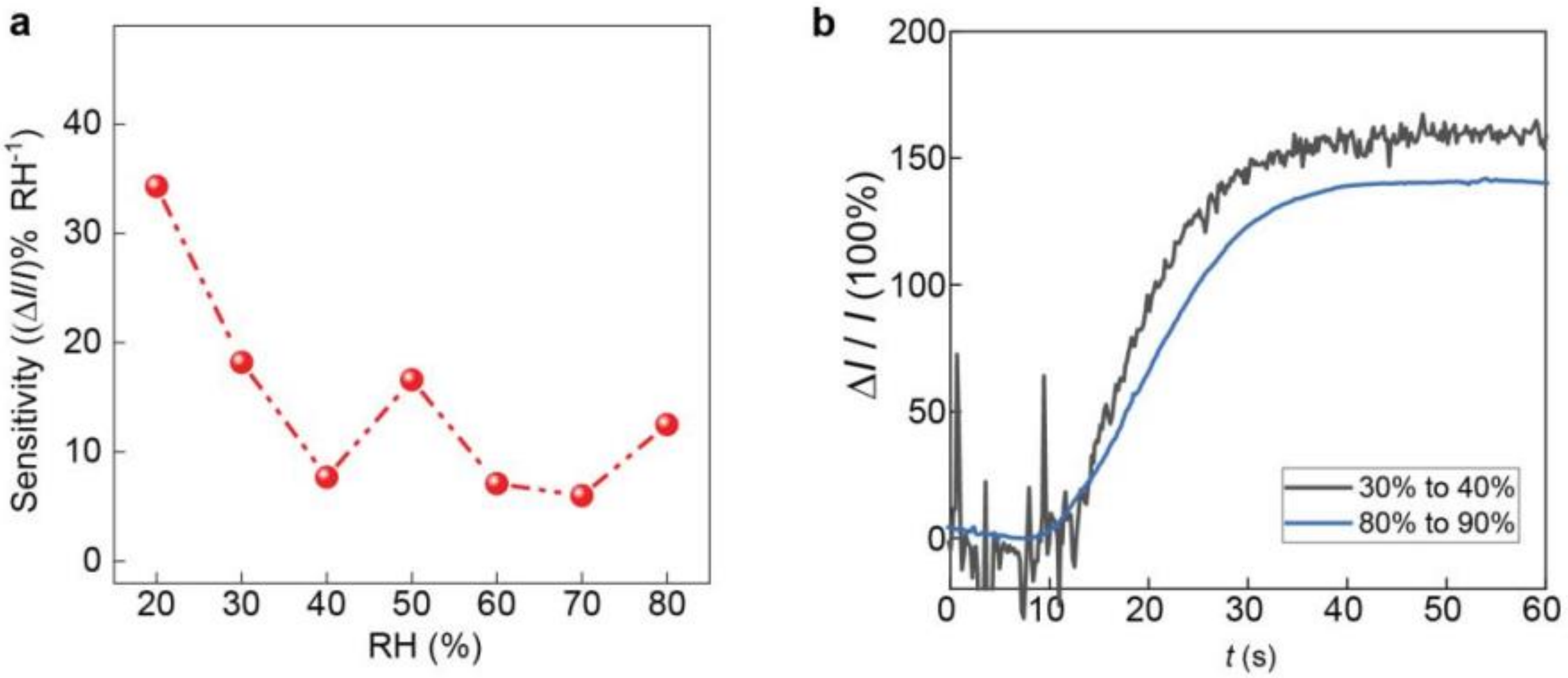

Sensor sensitivity at different relative humidity (RH). (**a**) Extrapolated (from Fig. 2a) sensor sensitivity, defined as the percentage change in conductance per percentage change in RH ((Δ*I*/*I*)%·RH-1), at different RH baselines. The protein nanowire sensor maintained a sensitivity > 6%·RH-1. (**b**) Real-time sensor responses to a 10% RH change at the baseline RH of 30% (gray) and 80% (blue), respectively. The sensor showed similar response at the low and high RH baselines, consistent with extrapolated sensitivity in (a)

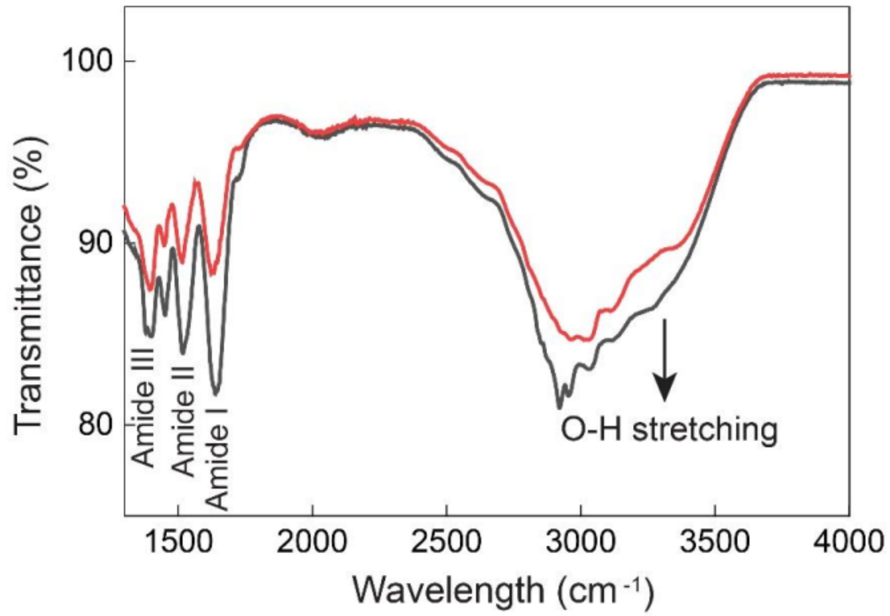

FTIR spectra of protein nanowire films at relative humidity (RH) of 20% (red curve) and 40% (gray curve). The broad peak ~3400 cm^{-1} corresponds to the O-H stretching band in free water,[9] and the increased intensity (gray curve) indicates increased water adsorption in the film at higher relative humidity. The increased intensities in other peaks could be caused by protein segments that became more mobile after moisture filling interstitial void.

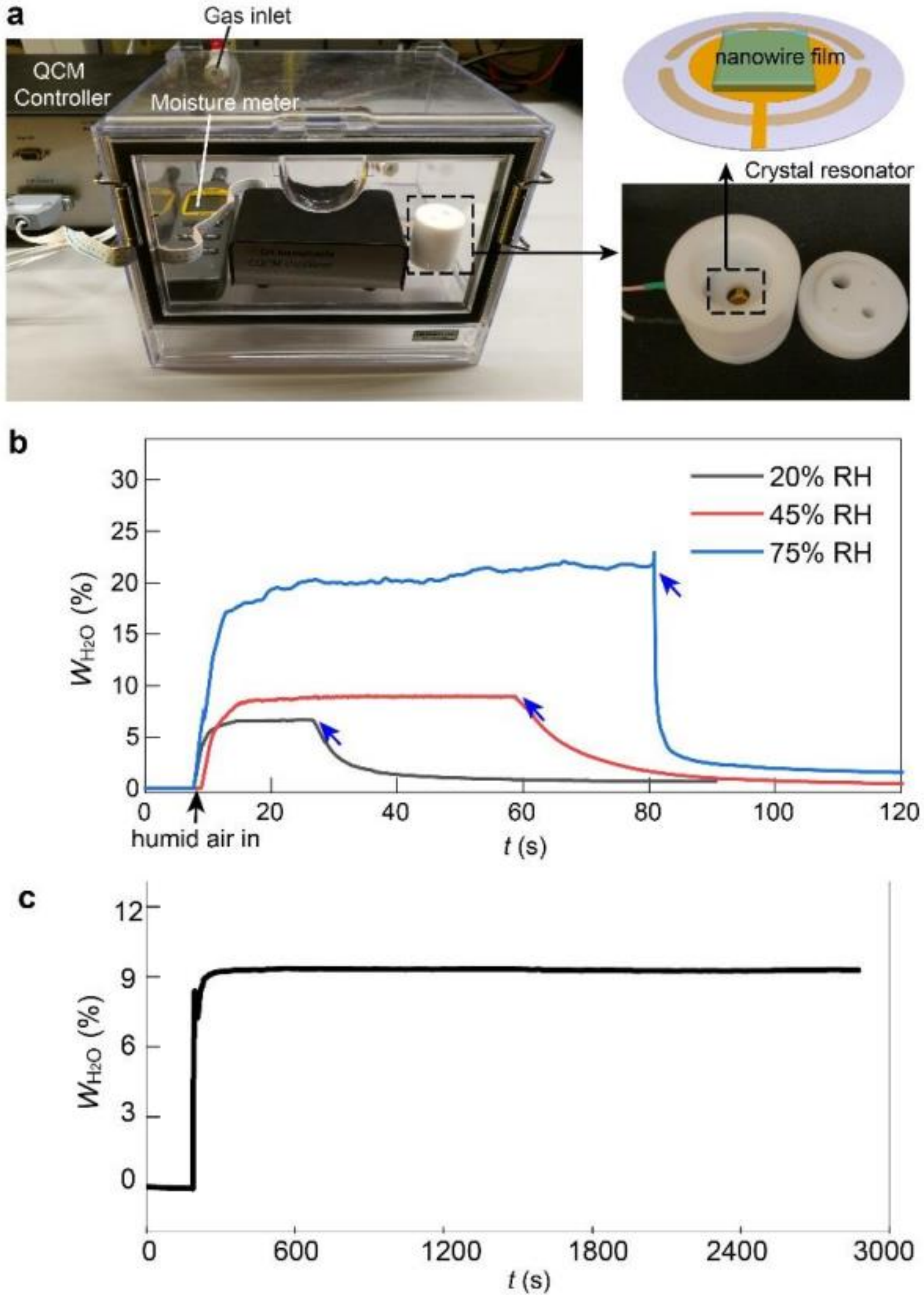

The adsorbed moisture was measured to be stable in the protein nanowire film at fixed RH (~40%).

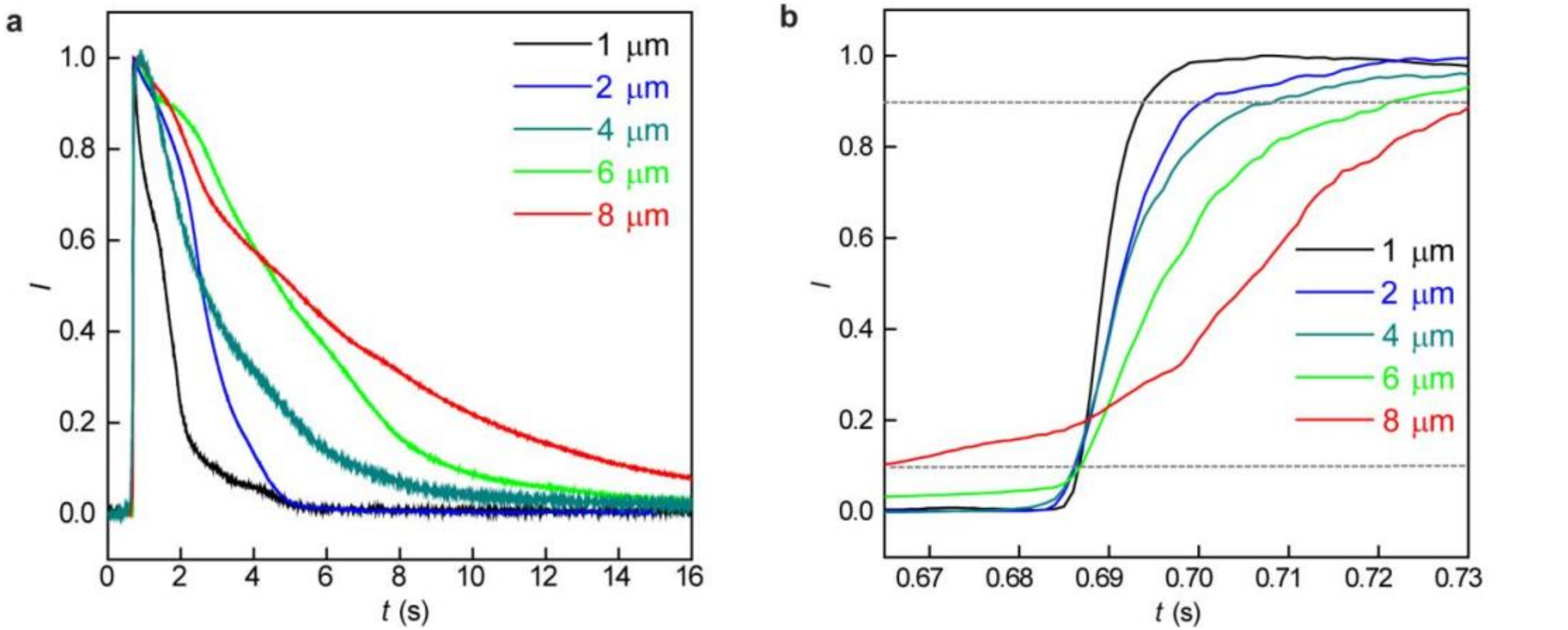

Thickness-dependent sensor response. (**a**) The sensor response to an instant increase of RH from 30% to 90% and instant removal. The decay times, defined as the time for the signal to reduce to 10% of the peak value, were 2.1 s, 2.9 s, 7.4 s, 12.4 s, and 15.3 s for nanowire film thickness of 1 μm, 2 μm, 4 μm, 6 μm, and 8 μm, respectively. (**b**) The response times, defined as the rising time from a 10% to 90% signal change (dashed lines), were 7 ms, 14 ms, 23 ms, 37 ms, and 69 ms for nanowire film thickness of 1 μm, 2 μm, 4 μm, 6 μm, and 8 μm, respectively.

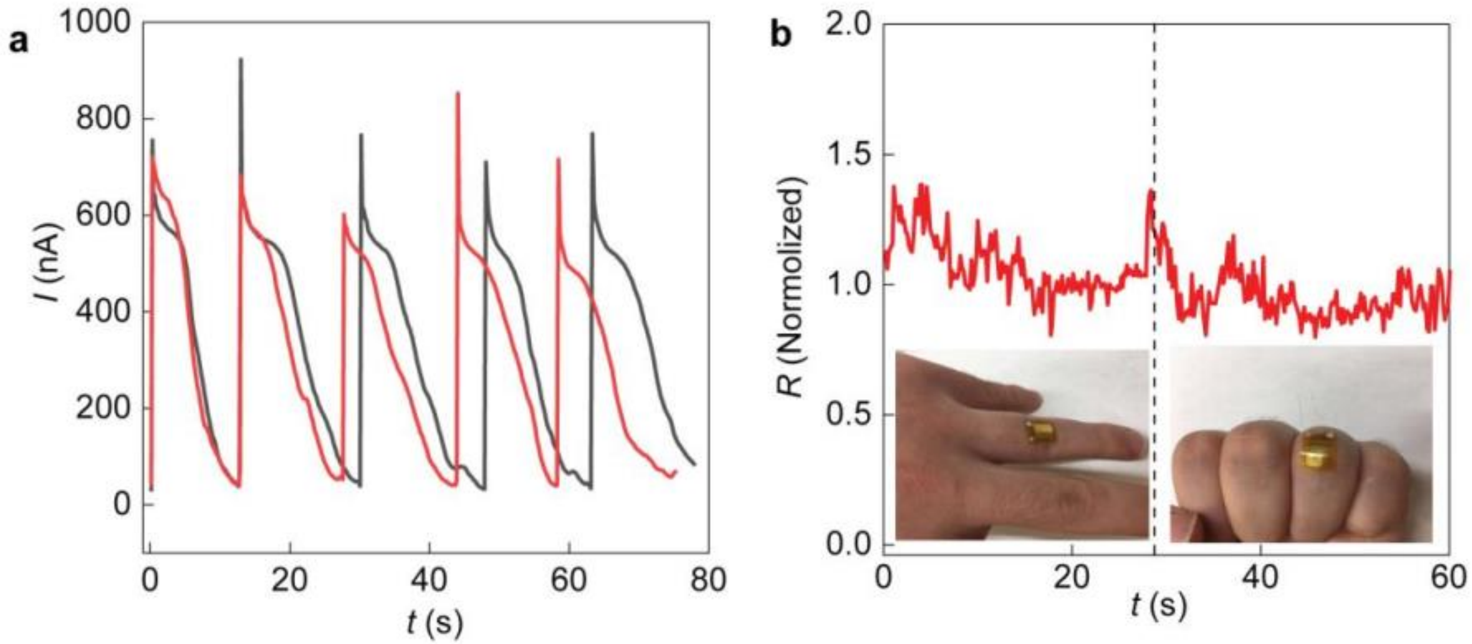

Mechanical testing. (**a**) The sensor response with respect to the repeated change of relative humidity (RH) between 45% and 92% in flat (black) and bending (red) state (with the bending radius of 0.5 mm). (**b**) Continuous monitoring of the (normalized) resistance in a protein nanowire sensor attached to a finger joint, before (left) and after (right) finger bending. T hesignal fluctuations largely came from local RH variations during the movements.

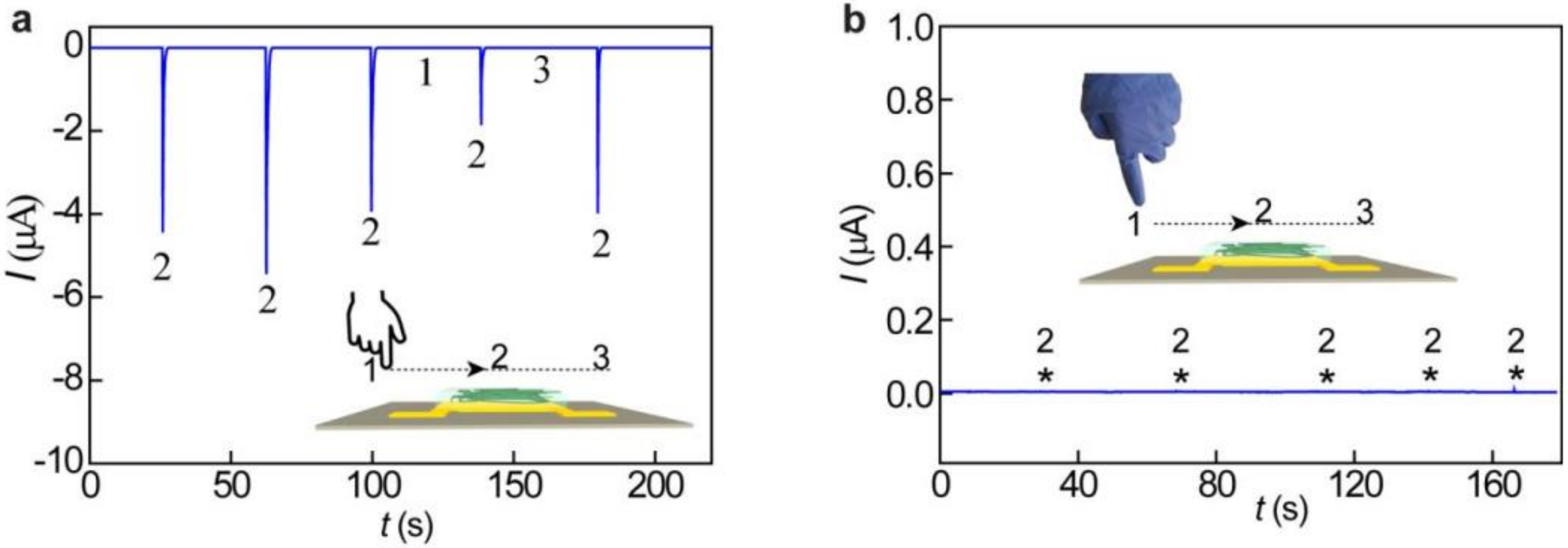

Sensor responses from moving fingers. (**a**) Current responses from a protein nanowire device to repeated (5 times) finger movements of swiping across. The bias voltage was flipped (V_{bias} = -1 V) from that in Fig. 3d. The inset shows the schematic of the finger track, with the numbers indicating the positions. (**b**) Current responses from a protein nanowire device to repeated (5 times) finger movements of swiping across, with the finger wearing a glove.

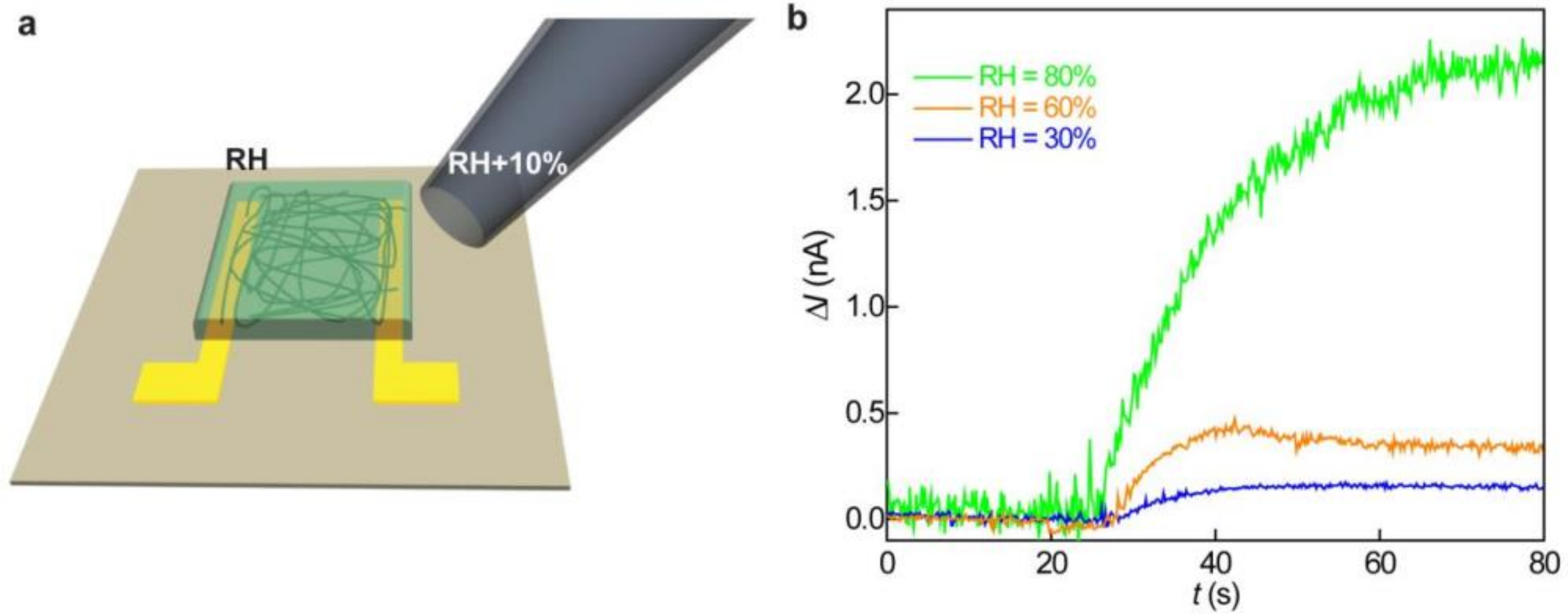

Humidity-dependent powerless sensing. (**a**) Schematic of the experimental setup to control the humidity difference between the two electrodes. The protein nanowire device was first exposed to a stable relative humidity (RH) background. Air of higher RH (*e.g.*, ΔRH = 10%) was then blew from one side to increase the local RH at one electrode. During the process, the current output (Δ*I*) from the device was monitored, with no external voltage applied. Both the background and flowing RHs were controlled by equilibrium vapor pressure of sulfuric acid solutions.[5] (**b**) Generated current (Δ*I*) at different background RH of 30%, 60%, and 80%. A trend of increasing current signal was observed with the increase in background RH.

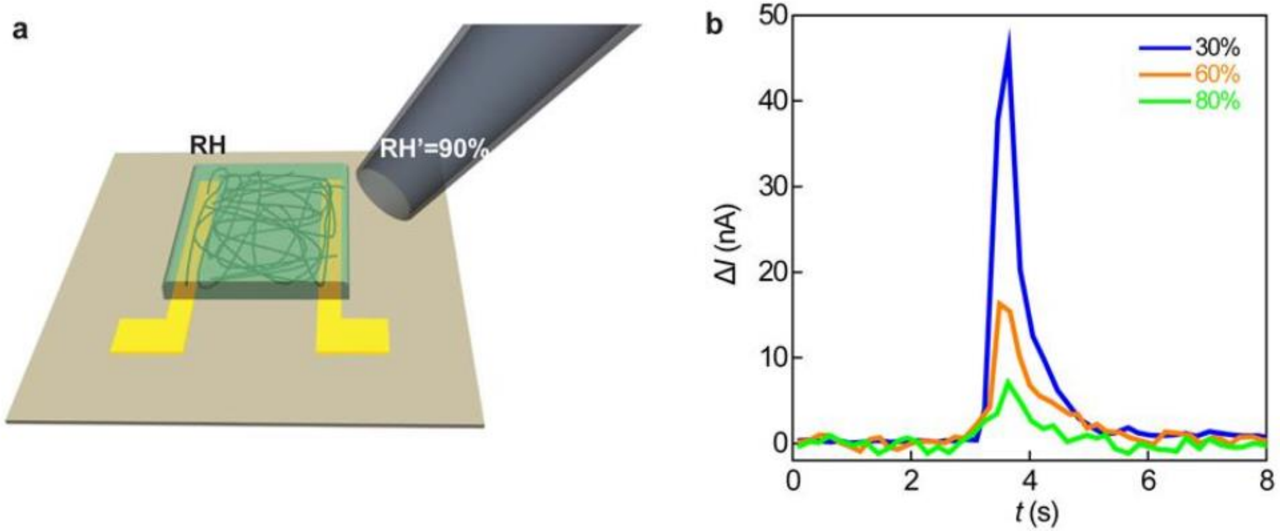

Humidity-dependent powerless sensing. (**a**) For practical wearable application (*e.g.*, breathing detection), usually the peak of the instant RH' is fixed independent of the background/ambient RH. We experimentally emulated breathing by flowing air (RH'~90%) from one side of the device to create instant humidity gradient. (**b**) Generated current (ΔI) at different background RH of 30%, 60%, and 80%. A trend of decreasing current signal was observed with the increase in background RH.

Conclusion

- The high-performance humidity sensing demonstrated here has potential applications in physiological monitoring and remote body tracking.
- The outer surface of e-PNs can be functionalized peptide ligands designed to specifically bind analytes of interest.

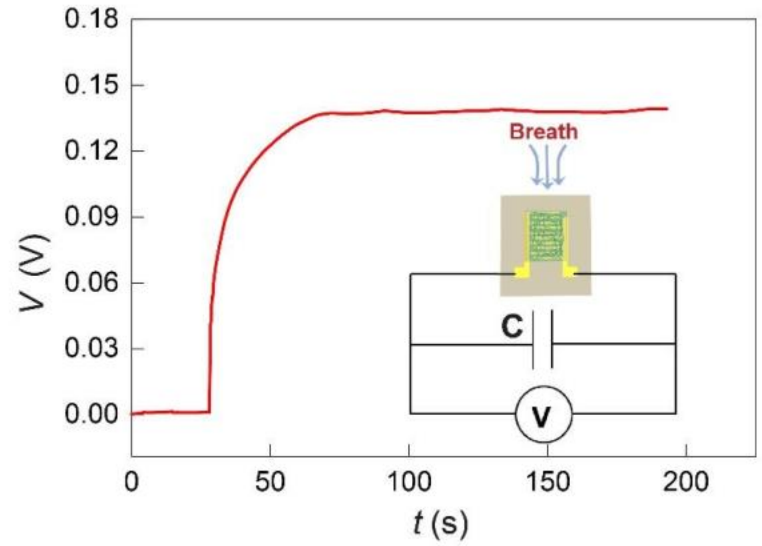

Electric power generation. Instant humidity gradient in percolative conductive films was shown to yield electric potential gradient and hence a measured voltage output. Here we demonstrated that the protein nanowire device could generate a ~0.13 V output voltage by a humidity gradient induced by a breath, which could be used to charge up a capacitor (10 µF).